Renormalization of the electron-phonon interaction by strong electronic correlations in high-T_c superconductors

Roland Zeyher
Max-Planck-Institut für Festkörperforschung, 70569 Stuttgart, Germany

Miodrag L. Kulić
Max-Planck-Institut für Festkörperforschung, 70569 Stuttgart, Germany
and 2. Physikalisches Institut, Universität Stuttgart, 70563 Stuttgart, Germany

(Received 1 May 1995)

The renormalization of the electron-phonon interaction by strong electronic correlations is studied using a one-band Hubbard model with infinite repulsion and nearest (t model) and nearest and second-nearest (tt' model) neighbor hopping terms and an on-site electron-phonon coupling. Using Hubbard's X operators and an extension from 2 to N degrees of freedom for the electrons the leading contributions for the electron self-energy and the vertex function in $1/N$ and the electron-phonon coupling constant are given and numerically evaluated for a square lattice. We find that the momentum dependence of the vertex function depends strongly on doping: For large dopings it is rather weak, with decreasing doping it becomes more and more pronounced leading to a strong reduction of the vertex at larger momentum transfers until, for very small dopings, the vertex essentially consists of a forward scattering peak with a width proportional to the doping. This behavior occurs both in the t and the tt' models and also in one dimension where analytic expressions are derived. Correlation effects also change α^2F in general: The full-symmetric component α^2F_1 is in the t model somewhat, in the tt' model rather strongly suppressed, especially near half-filling; the other symmetry components α^2F_i with $i=2,...,5$ increase strongly with decreasing doping and are of similar magnitude as α^2F_1 near half-filling. Including also direct Coulomb repulsion nontrivial symmetries such as d wave become more stable than the s-wave order parameter below a critical value for the doping even for the considered phonon-mediated superconductivity. Most dramatic, however, is the quenching of the resistivity due to electron-phonon scattering both in the t and the tt' models at intermediate and small dopings. This result may explain the absence of phonon features in the experimental transport coefficients of high-T_c compounds.

I. INTRODUCTION

Strong correlations between electrons and a non-negligible electron-phonon interaction are two characteristic features of high-T_c oxides. The relevance of correlations in these compounds is well documented: Self-consistent band-structure calculations as well as photoemission experiments find an effective Hubbard constant U for the Cu ions of about 6–10 eV,[1,2] which is much larger than the observed width of the conduction bands of about 1 eV.[3] A rather direct evidence for strong correlations also comes from the doping dependence of the frequency-dependent conductivity[4] in $La_{1-x}Sr_xCuO_4$ and $YBa_2Cu_3O_{7-x}$, in particular, from the observed shift of spectral weight from large to low energies with doping.[5]

There is also good evidence that the bare electron-phonon coupling in high-T_c oxides is not small: Self-consistent local-density approximation band-structure calculations yield a rather large electron-phonon coupling constant $\lambda \sim 1$–1.5.[6,7] Experimentally, superconductivity-induced phonon renormalizations,[8] Fano line shapes,[8] large isotope coefficients away from optimal doping,[9] and phonon-related features in tunneling spectra[10,11] give evidence for a substantial electron-phonon coupling in these compounds. On the other hand, if the data are interpreted only in terms of a strong electron-phonon coupling some puzzles arise. One is connected with the conductivity: In optimally doped systems the width of the Drude peak and the temperature dependence of the resistivity are not incompatible with a strong-coupling theory using $\lambda \sim 3$ and $\lambda_{tr} \sim 1$, where λ_{tr} is the transport electron-phonon coupling constant.[12] However, the same theory would require $\lambda \sim \lambda_{tr} < 0.1$ in the overdoped system $Bi_{2+x}Sr_{2-y}CuO_{6\pm\delta}$,[13] which seems to be incompatible with the band-structure results. Furthermore, it is even doubtful whether at all the electron-phonon scattering determines the conductivity in this system as well as in doped $La_{1-x}Sr_xCuO_4$:[14] The experimental curves do not show any features at low temperatures which could be associated with a transition to the asymptotic T^5 law of phonon scattering. Moreover, the rather continuous evolution of the resistivity $\rho(T)$ as function of doping questions the early interpretations of the linear dependence of ρ in optimal doped systems in terms of phonon scattering. Thus a pure electron-phonon theory is confronted with the problem to explain why the electron-phonon coupling is present in self-energy effects but absent in transport properties or, equivalently, why λ_{tr} is much smaller than λ.[15] One possibility is that correlation effects strongly renormalize the electron-phonon coupling.[16–19] It is the aim of this paper to investigate this problem in a controlled and quantitative way.

The important low-energy physics of electrons in high-T_c oxides can be described in a good approximation by a one-band Hubbard model on a square lattice.[1,2] Exact diagonalization studies of small clusters suggest that the charge-

fluctuation spectra vary only weakly at large U's.[20] Since we are dealing in the following only with charge fluctuations we thus may put U equal to infinity. The resulting electronic model is called a t (tt') model if nearest (nearest and second-nearest) neighbor hopping terms are included. These two models will be studied in the following. As to the electron-phonon interaction, there are two kinds of couplings: First, there is an ioniclike, site-diagonal coupling where the total electronic density at a lattice site interacts with phonons; second, there is a covalentlike, site-nondiagonal coupling where the dependence of the hopping matrix elements on the distance between the sites causes the coupling. The perturbation expansion for the two types of couplings is different and somewhat simpler for the first type. Since there are also reasons to believe that the ioniclike coupling dominates in high-T_c oxides,[7,21] we will consider only this coupling in the following.

The Hamiltonian of our electron-phonon model is given in Sec. II in terms of Hubbard's X operators. Instead of one orbital per site we introduce $N/2$ identical orbitals per site and generalize the Hamiltonian correspondingly treating later $1/N$ as a small parameter. We also specify carefully the Hilbert space and the action of the X operators on its states. The most popular way to proceed would be to decompose the X operators into products of Fermi and Bose operators which obey the usual simple commutation rules. The resulting slave-boson or fermion treatments[22–24] are characterized by an increase of degrees of freedom plus constraints, local gauge symmetries which are often broken on the mean-field level, etc. In Sec. III we present a direct, slave-free Baym-Kadanoff perturbation expansion for the electron self-energy which uses the unmodified X operators and the original, unenlarged Hilbert space.[18,25] General, formally closed expressions for the electronic self-energy in the presence of a weak electron-phonon interaction will be given in this section. In Sec. IV we specialize to the case where the parameter $1/N$ is small. It is then sufficient to keep only the leading terms for the electronic self-energy and the vertex function for which explicit expressions will be given in the normal state. In this section the Eliashberg function $\alpha^2F(\omega)$ will be derived and decomposed in its irreducible symmetry components. It also will be compared with its usual form where correlation effects are neglected. All modifications due to correlations can be expressed by a few symmetry- and **q**-dependent functions, called enhancement functions in the following. In Sec. V our expression for the vertex will be compared with the corresponding one of the slave-boson method. Though our X operator approach has, for instance, no Bose condensate we will show that the two approaches give nearly, but not exactly the same results in leading order of the $1/N$ expansion. Whether such an approximate equivalence holds to all order in $1/N$ remains to be seen. Finally, Sec. VI contains exact results for the t model in one dimension and numerical results for the two-dimensional t and tt' models. Our conclusions can be found in Sec. VII. For readers who are not interested in the details of the derivations we would like to point out the most important expressions used in the numerical evaluation in Sec. VI: Eqs. (52)–(59) contain the various forms for the Eliashberg functions α^2F and Eqs. (41)–(44) explicit expressions for the vertex function.

Some aspects of the influence of correlation effects on the electron-phonon interaction have already been discussed in the literature.[16–19,26,27] In particular, the frozen phonon calculations in Refs. 16 and 17, using a covalentlike electron-phonon coupling, yielded results for a special, large-momentum phonon which are in line with our findings. Some of our results for the t model have already been published in Refs. 18, 26, and 27. The aim of this paper is to present the theory in more detail and to give complete numerical results, in particular, also for the tt' model.

II. HAMILTONIAN AND HILBERT SPACE

Our Hamiltonian reads

$$H=\sum_{\substack{i\\ p=0\ldots N}} E_{ip}X_i^{pp}-\sum_{\substack{ij\\ p=1\ldots N}}\frac{t_{ij}}{N}X_i^{po}X_j^{0p}+\sum_{\mathbf{k}\lambda}\omega(\mathbf{k}\lambda)\times\left(a^\dagger(\mathbf{k}\lambda)a(\mathbf{k}\lambda)+\frac{1}{2}\right)+\sum_{\substack{i\mathbf{k}\lambda\\ p=1\ldots N}} g_i(-\mathbf{k}\lambda)[a^\dagger(\mathbf{k}\lambda)+a(-\mathbf{k}\lambda)](X_i^{pp}-\langle X_i^{pp}\rangle). \quad (1)$$

The first two terms in Eq. (1) describe the electronic part of H; E_{ip} and t_{ij} are atomic energies at the atomic site i and hopping amplitudes between the sites i and j, respectively. It is assumed in the following that the atomic sites form a square lattice. X_i^{pq} is a Hubbard X operator for the atomic site i where $p,q=0$ refer to the empty and $p,q=1\ldots N$ to a singly occupied state with spin directions p,q. The first two terms in Eq. (1) are invariant under SU(N) transformations. Sometimes, for instance, in discussing superconductivity, it is more convenient to use a symplectic extension to N degrees of freedom: SU(N) is replaced by the symplectic group $Sp(N/2)$; the index p then consists of a spin-1/2 projection label and a flavor index counting the $N/2$ identical orbitals. The third term in Eq. (1) is the free phonon part where $a^\dagger(\mathbf{k}\lambda)$ creates a phonon with momentum $\mathbf{k}$, branch index λ, and frequency $\omega(\mathbf{k}\lambda)$. The fourth term in Eq. (1) represents the electron-phonon coupling with the coupling function g. It describes an ioniclike coupling where the phonons change the chemical potential locally at the lattice sites.[21] $\langle X_i^{pp}\rangle$ is the thermal average of X_i^{pp} and has to be introduced in the interaction to have $\langle a^\dagger(\mathbf{k}\lambda)\rangle=0$. The hopping terms t_{ij} in Eq. (1) have been scaled with $1/N$ so that the limit $N\to\infty$ is physically meaningful and the leading order of the self-energy is of $O(1)$.

For $N=2$ the Hamiltonian Eq. (1) describes usual spin-1/2 particles. The extension to a general N is useful in order to obtain a small parameter $1/N$ and has been introduced in Ref. 25 in the framework of X operators. For a complete specification of the problem we also have to specify the underlying Hilbert space. We assume that it is spanned by the eigenfunctions of the diagonal operators X_i^{pp} with $p=1\ldots N$:

$$X_i^{pp}|n_1,\ldots n_p,\ldots n_N;n_0\rangle=n_p|n_1,\ldots n_p,\ldots n_N;n_0\rangle. \quad (2)$$

Assuming that X_i^{pp} is still a projector for $p=1\ldots N$ the eigenvalues n_p may be either 0 or 1. Imposing also the generalized constraint

$$\sum_{p=0}^{N} X_i^{pp} = N/2, \tag{3}$$

n_0 is determined by $n_0 = N/2 - \sum_{p=1}^{N} n_p$. Since X^{00} is assumed to be a non-negative operator as in the physical case $N=2$ we must have $n_0 \geqslant 0$, i.e., only such sets of numbers $n_1 \ldots n_N$ are admitted which lead to a non-negative n_0.

The action of nondiagonal X operators on the states of the Hilbert space is defined by

$$X_i^{pq}|n_0; n_1 \ldots n_p \ldots n_q \ldots n_N\rangle = (-1)^{n_p + \cdots + n_{q-1}}|n_0; n_1 \ldots n_p + 1 \ldots n_q - 1 \ldots n_N\rangle, \tag{4}$$

$$X_i^{0p}|n_0; n_1 \ldots n_p \ldots n^N\rangle = \sqrt{n_0 + 1}(-1)^{n_1 + \cdots + n_{p-1}}|n_0 + 1; n_1 \ldots n_p - 1 \ldots n_N\rangle, \tag{5}$$

$$X_i^{p0}|n_0; n_1 \ldots n_p \ldots n_N\rangle = \sqrt{n_0}(-1)^{n_1 + \cdots + n_{p-1}} \times |n_0 - 1; n_1 \ldots n_p + 1 \ldots n_N\rangle. \tag{6}$$

In Eqs. (4)–(6) the convention is used that vectors on the right-hand sides in these equations with unacceptable arguments should be identified with the zero vector. In Eq. (4) we also assumed $p<q$ without loss of generality. From Eqs. (4)–(6) it follows that fermionic X operators obey the anticommuting and bosonic X operators the commuting relations of usual X operators, i.e., those of the unextended case $N=2$ (fermionic operators are X operators where exactly one zero appears in the two indices; all the remaining X operators are called bosonic). In contrast to that, the commutators of fermionic and the anticommutators of bosonic X operators depend explicitly on N. From Eqs. (4)–(6) follows, in particular, the identity

$$X^{00}X^{pq} = X^{00}\delta_{pq} - X^{0q}X^{po}. \tag{7}$$

It relates diagonal to nondiagonal elements of the X operators and will be used in Sec. IV to express expectation values of bosonic X operators in terms of Green's functions. Note that the left- and right-hand sides of Eq. (7) are identical zero in the case $N=2$.

Finally, we remark that the slave-boson representation of X operators for $p>0, q>0$:

$$X_i^{op} = b_i^\dagger f_{ip}, X_i^{pq} = f_{ip}^\dagger f_{iq}, X_i^{00} = b_i^\dagger b_i \tag{8}$$

in terms of bosonic and fermionic creation and destruction operators $b_i^\dagger, b_i$ and $f_{ip}^\dagger, f_{ip}$, respectively, also obeys Eqs. (4)–(6). Using such a representation one is, however, forced to introduce a Bose condensate $\langle b\rangle$ which has no analog in the X-operator approach. The reason for this is that in the Hilbert space where the X operators act the operators b or $b^\dagger$ are no admissible operators: Applying them to a state vector yields in general vectors which no longer belong to the Hilbert space.

III. THE ELECTRON SELF-ENERGY IN THE PRESENCE OF A WEAK ELECTRON-PHONON COUPLING

Using the Hamiltonian Eq. (1) the Heisenberg equation of motion for fermionic operators becomes

$$\left(\frac{\partial}{\partial \tau_1} - E(1)\right) X(1) = \int d2\, d3\, t(123) Y(2) X(3) + \int d\overline{2}\, d3 h(1\overline{23}) H(\overline{2}) Y(3). \tag{9}$$

$\overline{1}$ stands for the site i_1 and the imaginary time τ_1, $\overline{1} = (i_1 \tau_1)$. Similarly, 1 stands for 1 and the pair pq of internal labels, so that $1 \equiv \binom{pq}{1}$. The functions t and h are given explicitly by

$$t(123) = -\frac{t_{i_1 i_3}}{N}\delta_{i_1 i_2}\delta(\tau_1 - \tau_2)\delta(\tau_3 - \tau_1)[(\delta_{p_2 0}\delta_{q_1 q_2}\delta_{p_1 p_3} + \delta_{p_1 p_2}\delta_{q_2 p_3})\delta_{q_1 0}(1 - \delta_{p_3 0})\delta_{q_3 0} - (\delta_{p_2 q_3}\delta_{q_1 q_2} + \delta_{p_1 p_2}\delta_{q_2 0}\delta_{q_1 q_3})\delta_{p_1 0}(1 - \delta_{q_3 0})\delta_{p_3 0}], \tag{10}$$

$$h(1\overline{23}) = -\delta_{i_1 i_2}\delta_{i_1 i_3}\delta(\tau_1 - \tau_2)\delta(\tau_1 - \tau_3)(\delta_{p_1 0}\delta_{q_1 q_3}\delta_{p_3 0} - \delta_{q_1 0}\delta_{q_3 0}\delta_{p_1 p_3}). \tag{11}$$

Y denotes a bosonic X operator, a notation, which is often convenient to distinguish bosonic and fermionic X operators in an explicit way. $H(1)$ is given by

$$H(\overline{1}) = \sum_{\mathbf{k}\lambda} g_{i_1}(-\mathbf{k}\lambda)[a^\dagger(\mathbf{k}\lambda\tau_1) + a(-\mathbf{k}\lambda\tau_1)]. \tag{12}$$

Following Ref. 28 we define nonequilibrium Green's functions with fermionic Hubbard operators by

$$G\left(\begin{matrix} 0 q_1 & \mathrm{p}_2 0 \\ 1 & 2 \end{matrix}\right) = -\langle TSX^{0q_1}(\overline{1})X^{p_2 0}(\overline{2})\rangle / \langle S\rangle, \tag{13}$$

$$S = Te^{\Sigma_{p_2 q_2}\int d\overline{2} Y^{p_2 q_2}(\overline{2}) K^{p_2 q_2}(\overline{2})}. \tag{14}$$

$\int d\overline{1}$ means $\Sigma_{i_1}\int_0^\beta d\tau_1$. T is the time ordering operator, K an external source which couples to bosonic X operators. Using the equation of motion, Eq. (9), it is easy to show that G satisfies the Dyson equation

$$\sum_{q_2}\int d\overline{2}\left\{\delta(\overline{2} - \overline{1})\left[\delta_{q_2 q_1}\left(-\frac{\partial}{\partial \tau_2} + (E_{i_1 0} - E_{i_1 q_1})\right) - K^{00}(\overline{1})\delta_{q_1 q_2} + K^{q_1 q_2}(\overline{1})\right] - \Sigma\left(\begin{matrix} 0 q_1 & 0 q_2 \\ 1 & 2 \end{matrix}\right)\right\} G\left(\begin{matrix} 0 q_2 & p_1' 0 \\ 2 & 1' \end{matrix}\right) = \delta(\overline{1} - \overline{1'}) Q_{0 q_1, p_1' 0}(\overline{1}). \tag{15}$$

Q is given by

$$Q_{0q_1,p_1'0}(\overline{1})=\langle[X^{0q_1}(\overline{1}),X^{p_1'0}(\overline{1})]_+\rangle. \tag{16}$$

The self-energy Σ is defined by

$$\begin{aligned}\int d2\,\Sigma(12)G(21')=&\int d2\,d3t(123)\\&\times\frac{\langle TSY(2)X(3)X(1')\rangle}{\langle S\rangle}\\&+\int d\overline{2}\,d3h(1\overline{2}3)\\&\times\frac{\langle TSH(\overline{2})X(3)X(1')\rangle}{\langle S\rangle}.\end{aligned} \tag{17}$$

It is also convenient to introduce the normalized Green's function

$$\tilde{G}\left(\frac{0q_1}{1},\frac{0q_1'}{1'}\right)=\sum_{p'}G\left(\frac{0q_1}{1},\frac{p'0}{1'}\right)Q^{-1}_{p'0,0q_1'}(\overline{1'}). \tag{18}$$

$\tilde{G}$ satisfies Eq. (15) if Q on the right-hand side is replaced by $\delta_{q_1p_1'}$.

We now assume that the electron-phonon coupling is weak so that Σ can be expanded in a power series in g:

$$\Sigma(11')=\Sigma^{(0)}(11')+\Sigma^{(2)}(11')+\ldots, \tag{19}$$

where $\Sigma^{(i)}$ is of power i in g. $\Sigma^{(1)}$ vanishes in equilibrium and thus can be dropped. From the modified Dyson equation follows

$$\Sigma^{(2)}(11')=\int d2\,d3\tilde{G}^{-1}(12)\tilde{G}^{(2)}(23)\tilde{G}^{-1}(31') \tag{20}$$

where $\tilde{G}^{(i)}$ denotes terms of power i in g and $\tilde{G}^{(0)}$ is simply denoted by $\tilde{G}$. Carrying out second-order perturbation theory in Eq. (13) in the electron-phonon interaction one finds

$$G^{(2)}(23)=\frac{-1}{2}\int d\overline{4}\,d\overline{5}V(\overline{4}-\overline{5})\frac{\delta^2G(23)}{\delta K(\overline{4})\delta K(\overline{5})}. \tag{21}$$

$K(\overline{4})$ stands for $K(\overset{00}{4})$. V is the phonon-medited interaction

$$V(\overline{1-2})=\sum_{\mathbf{k}\lambda}g_{i_1}(-\mathbf{k}\lambda)D^{\rm ph}(\mathbf{k}\lambda,\tau_1-\tau_2)g_{i_2}(\mathbf{k}\lambda), \tag{22}$$

where $D^{\rm ph}$ denotes the phonon Green's function. From Eq. (18) follows

$$\begin{aligned}\frac{\delta^2G(23)}{\delta K(\overline{4})\delta K(\overline{5})}=&\frac{\delta^2\tilde{G}(23)}{\delta K(\overline{4})\delta K(\overline{5})}Q(3)+\tilde{G}(23)\frac{\delta^2Q(3)}{\delta K(\overline{4})\delta K(\overline{5})}\\&+\frac{\delta\tilde{G}(23)}{\delta K(\overline{4})}\frac{\delta Q(3)}{\delta K(\overline{5})}+\frac{\delta\tilde{G}(23)}{\delta K(\overline{5})}\frac{\delta Q(3)}{\delta K(\overline{4})}.\end{aligned} \tag{23}$$

Inserting Eq. (23) into Eqs. (20) and (21) one finds

$$\Sigma^{(2)}(11')=\frac{-1}{2}\int d2\,d3\,d\overline{4}\,d\overline{5}\tilde{G}^{-1}(12)V(\overline{4}-\overline{5})\left(\frac{\delta^2\tilde{G}(23)}{\delta K(\overline{4})\delta K(\overline{5})}+2\frac{\delta\tilde{G}(23)}{\delta K(\overline{4})}\frac{\delta Q(3)}{\delta K(\overline{5})}Q^{-1}(3)\right)\tilde{G}^{-1}(31'). \tag{24}$$

Defining the vertex function $\tilde{\Gamma}$ by

$$\tilde{\Gamma}(11';2)=\frac{\delta\tilde{G}^{-1}(11')}{\delta K(2)}, \tag{25}$$

the functional derivatives of $\tilde{G}$ with respect to K can be written as

$$\frac{\delta\tilde{G}(12)}{\delta K(\overline{5})}=-\int d6\,d7\tilde{G}(16)\tilde{\Gamma}(67;\overline{5})\tilde{G}(72), \tag{26}$$

$$\begin{aligned}\frac{\delta^2\tilde{G}(12)}{\delta K(\overline{4})\delta K(\overline{5})}=&\int d6\,d7\,d8\,d9\tilde{G}(18)\tilde{\Gamma}(89;\overline{4})\tilde{G}(96)\tilde{\Gamma}(67;\overline{5})\tilde{G}(72)-\int d6\,d7\tilde{G}(16)\frac{\delta\tilde{\Gamma}(67;\overline{5})}{\delta K(\overline{4})}\tilde{G}(72)\\&+\int d6\,d7\,d8\,d9\tilde{G}(16)\tilde{\Gamma}(67;\overline{5})\tilde{G}(78)\tilde{\Gamma}(89;\overline{4})\tilde{G}(92).\end{aligned} \tag{27}$$

Inserting Eq. (27) into Eq. (24) yields finally

$$\begin{aligned}\Sigma^{(2)}(11')=-\int d\overline{4}\,d\overline{5}V(\overline{4}-\overline{5})\Bigg(&\int d6\,d7\tilde{\Gamma}(16;\overline{4})\tilde{G}(67)\tilde{\Gamma}(71';\overline{5})-\frac{1}{2}\frac{\delta\tilde{\Gamma}(11';\overline{5})}{\delta K(\overline{4})}\\&-\int d6\,d7\tilde{\Gamma}(16;\overline{4})\tilde{G}(67)\frac{\delta Q(7)}{\delta K(\overline{5})}Q^{-1}(7)\tilde{G}^{-1}(71')\Bigg).\end{aligned} \tag{28}$$

The expression for the zeroth-order self-energy $\Sigma^{(0)}_{\text{can eas Y}}$ in the average over three operators by a functional derivative with respect to K, and by using then Eq. (25). The result is

$$\Sigma^{(0)}(11')=-\int d2\,t(121')\langle Y(2)\rangle + \int d2\,d3\,d4\,t(123)\tilde{G}(34)\tilde{\Gamma}(41';2) - \int d2\,d3\,d4\,t(123)\tilde{G}(34)\,\frac{\delta Q(4)}{\delta K(2)} \times Q^{-1}(4)\tilde{G}^{-1}(41'). \tag{29}$$

Equations (28) and (29) are the main results of this section: They give explicit expression for the electron self-energy in the presence of a weak electron-phonon interaction in terms of $\tilde{G}$, $\tilde{\Gamma}$, and the derivative $\delta\tilde{\Gamma}/\delta K$ which are to be calculated without the electron-phonon coupling. Note also that Eqs. (28) and (29) are valid in the presence of a source field K. Equation (28) tells us that only charge fluctuations enter $\Sigma^{(2)}$ because the third, bosonic argument of $\tilde{\Gamma}$ always has the internal pair index 00. This is a consequence of our Hamiltonian Eq. (1) where phonons only couple to density fluctuations.

IV. DETERMINATION OF THE VERTEX FUNCTION IN $O(1)$

In the Baym-Kadanoff theory Σ is considered as a functional of $\tilde{G}$ and Q but does not depend explicitly on the source field K. Using this, the definition of $\tilde{\Gamma}$, Eq. (25), and Dyson's equation we obtain

$$\tilde{\Gamma}(11';2)=-\frac{\delta W(11')}{\delta K(2)}+\int d3\,d4\,d5\,d6\,\frac{\delta\Sigma^{(0)}(11')}{\delta\tilde{G}(34)} \times\tilde{G}(35)\tilde{\Gamma}(56;2)\tilde{G}(64) - \int d3\,\frac{\delta\Sigma^{(0)}(11')}{\delta Q(3)}\,\frac{\delta Q(3)}{\delta K(2)}. \tag{30}$$

$W(11')$ is the inverse of $\tilde{G}^{(0)}(11')$. The derivative of $\tilde{G}$ with respect to K in the second term on the right-hand side has been expressed by $\tilde{\Gamma}$ by taking the derivative of the identity $\tilde{G}\tilde{G}^{-1}=1$. Finally we have to relate Q, or, equivalently, $\langle Y^{pq}(1)\rangle$, to $\tilde{G}$. Taking the expectation value of the operator identity Eq. (7) in the presence of the source field K we obtain the general relation

$$\langle Y^{pq}(\bar{1})\rangle=\tilde{G}\begin{pmatrix}0p & 0q\\ \bar{1} & \bar{1}^{+}\end{pmatrix}-\frac{\delta\langle Y^{pq}(\bar{1})\rangle}{\delta K^{00}(\bar{1})}\,\frac{1}{\langle X^{00}(\bar{1})\rangle} \sum_{q'}\tilde{G}\begin{pmatrix}0p & 0q'\\ \bar{1} & \bar{1}^{+}\end{pmatrix}\frac{\langle Y^{pq'}(\bar{1})\rangle}{\langle X^{00}(\bar{1})\rangle}-\frac{\langle Y^{pq}(\bar{1})\rangle}{\langle X^{00}(\bar{1})\rangle},$$

where $\overline{1^{+}}$ denotes $\overline{1}$ with an infinitesimally increased time argument. Equations (29)–(31) form a closed system of equations for the self-energy, the vertex function, and the expectation values of Y operators in the presence of a source field K.

Without any approximation we can make the following two simplifications in Eqs. (29)–(31) in the normal state.

(a) In the absence of superconductivity the two pairs of internal labels pq and $p'q'$ for fermionic operators in the Green's function, the self-energy, and the vertex function must have the form $p=p'=0$, $q\neq 0$, $q'\neq 0$ or $q=q'=0$, $p\neq 0$, $p'\neq 0$. Moreover, each of the two choices leads to the same closed system of equations so that we can confine ourselves to the first choice.

(b) For our purposes it is sufficient to consider only the source field $K^{00}(\bar{1})$. This means that the source field does not lower the symmetry of the Hamiltonian so that all selection rules without field can also be used in the presence of the above special source field:

$$\tilde{G}\begin{pmatrix}0q & 0q'\\ \bar{1} & \bar{1}'\end{pmatrix}=\delta_{qq'}\tilde{G}(\overline{1\,1'}), \tag{32}$$

$$\Sigma\begin{pmatrix}0q & 0q'\\ \bar{1} & \bar{1}\,\bar{1}'\end{pmatrix}=\delta_{qq'}\Sigma(\overline{1\,1'}), \tag{33}$$

$$\tilde{\Gamma}\begin{pmatrix}0q & 0q' & ; & 00\\ \bar{1} & \bar{1} & ; & \bar{5}\end{pmatrix}=-\delta_{qq'}\tilde{\Gamma}(\overline{1\,1'};\bar{5}). \tag{34}$$

In Eq. (34) we have introduced a minus sign in order to conform with the definition of the vertex in Ref. 18.

Finally we use $1/N$ as a small parameter to simplify the above equations. For the leading order it follows from Eqs. (3) and (15) that $\langle Y^{11}\rangle\sim O(1)$, $\langle X^{00}\rangle\sim O(N)$, $\tilde{G}\sim\Sigma\sim O(1)$. Iterating Eq. (31) we obtain

$$\langle Y^{11}(\bar{1})\rangle=\tilde{G}(\overline{1\,1^{+}})+O(1/N). \tag{35}$$

Taking a derivative of this relation we find

$$\frac{\delta Q(\bar{3}^{00})}{\delta K(\bar{2}^{00})}=-N\,\frac{\delta\tilde{G}(\bar{3}^{01}\,\bar{3}^{01}_{+})}{\delta K(\bar{2}^{00})}+O(1) =N\int d\bar{4}\,d\bar{5}\tilde{G}(\overline{3\,4})\tilde{\Gamma}(\overline{4\,5;2})\tilde{G}(\overline{5\,3^{+}})+O(1). \tag{36}$$

To calculate $\Sigma^{(0)}$ in Eq. (29) in $O(1)$ it is sufficient to use just the first term for $\tilde{\Gamma}$ on the right-hand side of Eq. (30) so that

$$\Sigma^{(0)}(\overline{1\,1'})=+\delta(\bar{1}-\bar{1}')\int d\bar{2}\,t(\bar{1}-\bar{2})\tilde{G}(\bar{2}^{+}\bar{1})-t(\bar{1}-\bar{1}') \times\langle X^{00}(\bar{1})\rangle+O(1/N). \tag{37}$$

$t(\bar{1}-\bar{2})$ is given by

$$t(\bar{1}-\bar{2})=t_{i_1i_2}\delta(\tau_1-\tau_2)/N. \tag{38}$$

It is sufficient to use only the first two terms in Eq. (37) in carrying out the derivatives of $\Sigma^{(0)}$ in Eq. (30). From Eq. (36) and Eqs. (32)–(34) the following equation for the vertex function is then obtained:

$$\tilde{\Gamma}(\overline{1\ 1'};\overline{2})=\delta(\overline{1}-\overline{1'})\,\delta(\overline{1}-\overline{2})+N\int d3\,d4\,d5[\,\delta(\overline{1}-\overline{1'})t(\overline{1}-\overline{3})+t(\overline{1}-\overline{1'})\,\delta(\overline{1}-\overline{3})]\tilde{G}(\overline{3\ 4})\tilde{\Gamma}(\overline{4\ 5;2})\tilde{G}(\overline{5\ 1^{+}}). \quad (39)$$

A more detailed proof that Eqs. (37) and (39) indeed represent the leading expressions for large N's is given in Ref. 34.

The vertex equation (39) can be solved exactly without source field K^{00}. Writing $\tilde{\Gamma}(1\,1';3)=\gamma(1-1',1-3)$ and performing Fourier transformations with respect to space and time variables Eq. (39) becomes

$$\gamma(k,q)=1+\frac{TN}{N_c}\sum_{k_1}[t(k)+t(k_1+q)]\tilde{G}(k_1)\times\tilde{G}(k_1+q)\,\gamma(k_1,q) \quad (40)$$

with $k=(\mathbf{k},i\omega_{n_1})$ and $q=(\mathbf{q},i\nu_n)$. N_c is the number of primitive cells. Equation (40) represents an integral equation with two separable kernels and thus can be solved:

$$\gamma(k,q)=\frac{1+b(q)-a(q)t(\mathbf{k})}{[1+b(q)][1+b(-q)]-a(q)c(q)}, \quad (41)$$

where

$$a(q)=v_c\int\frac{d^2k}{(2\pi)^2}\,\frac{f(\xi(\mathbf{k}))-f(\xi(\mathbf{k}+\mathbf{q}))}{\xi(\mathbf{k}+\mathbf{q})-\xi(\mathbf{k})-i\nu_n}, \quad (42)$$

$$b(q)=v_c\int\frac{d^2k}{(2\pi)^2}\,t(\mathbf{k})\,\frac{f(\xi(\mathbf{k}))-f(\xi(\mathbf{k}+\mathbf{q}))}{\xi(\mathbf{k}+\mathbf{q})-\xi(\mathbf{k})-i\nu_n}, \quad (43)$$

$$c(q)=v_c\int\frac{d^2k}{(2\pi)^2}\,t(\mathbf{k})t(\mathbf{k}+\mathbf{q})\,\frac{f(\xi(\mathbf{k}))-f(\xi(\mathbf{k}+\mathbf{q}))}{\xi(\mathbf{k}+\mathbf{q})-\xi(\mathbf{k})-i\nu_n}. \quad (44)$$

v_c is the area of the primitive cell and the $\mathbf{k}$ integrations in Eqs. (42)–(44) are to be extended over the first Brillouin zone. $\xi(\mathbf{k})$ is equal to $\epsilon(\mathbf{k})-\mu$ where $\epsilon(\mathbf{k})$ are the renormalized one-particle energies due to $O(1)$ terms in $\Sigma^{(0)}$ of Eq. (37). Furthermore, the first term in Eq. (37) can be absorbed into the chemical potential. In order to have the usual Hamiltonian for $N=2$ in Eq. (1) one has to put $t_{ij}=2t$ and $t_{ij}=2t'$ if i and j denote nearest- and second-nearest neighbors, respectively. For a square lattice we obtain then for the one-particle energies $\epsilon(\mathbf{k})=-q_0[\cos(k_x)+\cos(k_y)+8t'\cos(k_x)\cos(k_y)]$ choosing $4t$ and a as the energy and length units, respectively. a is the lattice constant of the square lattice, and $q_0=\delta/2$ where δ is the doping defined at $T=0$ by $1-\delta=2\int_{-\infty}^{\mu}N(\epsilon)d\epsilon$ and $N(\epsilon)$ is the density of renormalized one-particle states for one spin direction.

In order to determine $\delta\tilde{\Gamma}/\delta K$, which appears in Eq. (28), we take the derivative in the general vertex equation Eq. (39):

$$\frac{\delta\tilde{\Gamma}(\overline{1\ 1'};\overline{5})}{\delta K(\overline{4})}=F(\overline{1\ 1'},\overline{4\ 5})+\int d\overline{3}\,d\overline{6}\,d\overline{7}[\,\delta(\overline{1}-\overline{1'})t(\overline{1}-\overline{3})+t(\overline{1}-\overline{1'})\,\delta(\overline{1}-\overline{3})]\tilde{G}(\overline{3\ 6})\frac{\delta\tilde{\Gamma}(\overline{6\ 7;5})}{\delta K(\overline{4})}\tilde{G}(\overline{7\ 3^{+}}) \quad (45)$$

with the inhomogeneous term

$$F(\overline{1\ 1';4\ 5})=-\int d\overline{3}\,d\overline{6}\,d\overline{7}\,d\overline{8}\,d\overline{9}[\,\delta(\overline{1}-\overline{1'})t(\overline{1}-\overline{3})+t(\overline{1}-\overline{1'})\,\delta(\overline{1}-\overline{3})][\tilde{G}(\overline{3\ 8})\tilde{\Gamma}(\overline{8\ 9;4})\tilde{G}(\overline{9\ 6})\tilde{\Gamma}(\overline{6\ 7;5})\tilde{G}(\overline{7\ 3^{+}})+\tilde{G}(\overline{3\ 6})\tilde{\Gamma}(\overline{6\ 7;5})\tilde{G}(\overline{7\ 8})\tilde{\Gamma}(\overline{8\ 9;4})\tilde{G}(\overline{9\ 3^{+}})]. \quad (46)$$

In Eq. (46) we have expressed $\delta\tilde{G}/\delta K$ in terms of the vertex function as previously. Multiplying Eq. (45) with $V(4-5)$ and integrating over 4 and 5 one obtains a separable integral equation for the quantity

$$\sigma(\overline{1\ 1'})=\frac{1}{2}\int d\overline{4}\,d\overline{5}V(\overline{4}-\overline{5})\,\frac{\delta\tilde{\Gamma}(\overline{1\ 1';5})}{\delta K(\overline{4})}, \quad (47)$$

which can be solved trivially and which, according to Eq. (28), represents exactly the self-energy contribution. The result is

$$\sigma(\overline{1\ 1'})=\frac{A}{B}\left(\,\delta(\overline{1}-\overline{1'})\int d\overline{3}t(\overline{1}-\overline{3})+t(\overline{1}-\overline{1'})\right) \quad (48)$$

with the numbers

$$A=\int d\overline{4}\,d\overline{5}\,d\overline{6}\,d\overline{7}\,d\overline{8}\,d\overline{9}V(\overline{4}-\overline{5})\times\tilde{G}(\overline{3\ 8})\tilde{\Gamma}(\overline{8\ 9;4})\tilde{G}(\overline{9\ 6})\tilde{\Gamma}\overline{6\ 7;5})\tilde{G}(\overline{7\ 3^{+}}), \quad (49)$$

$$B=1-\int d\overline{1}\,d\overline{1'}\tilde{G}(\overline{2\ 1})\Big(\,\delta(\overline{1}-\overline{1'})\int d\overline{3}t(\overline{1}-\overline{3})+t(\overline{1}-\overline{1'})\Big)\tilde{G}(\overline{1'2^{+}}). \quad (50)$$

For a square lattice holds

$$\int d\overline{3}t(\overline{1}-\overline{3})=2+8t'. \quad (51)$$

According to Eq. (48) σ represents a static renormalization of the chemical potential (first term) and of the hopping matrix elements (second term) due to the electron-phonon interaction. These frequency-independent renormalizations can be neglected if $A/B \ll 1/2 - q_0$ which always holds with our assumptions except in the special case of exactly half-filling.

The third term for $\Sigma^{(2)}$ in Eq. (28) is due to first-order changes in $\tilde{G}$ and Q. Using Eq. (36) it is evident that its last factor, $\tilde{G}^{-1}$, is not compensated by a preceding factor $\tilde{G}$. This means that this term actually is not a self-energy term but a contribution to $\tilde{G}$ which should be kept on the right-hand side in Dyson's equation. It thus renormalizes the 1 in an additive way making the right-hand side of Dyson's equation frequency and momentum dependent. Being of order g^2 its real part may be neglected compared to 1 but its imaginary part contributes, for instance, to the amplitude of quasiparticles. We will not discuss this term further in this paper but concentrate on the first term in Eq. (28) which we denote by Σ_F. Carrying out obvious integrations[29] and assuming a slowly varying density of states near the Fermi energy we obtain

$$\Sigma_F(\mathbf{k}z) = \int_0^\infty d\omega \langle \alpha^2 F(\mathbf{k},\mathbf{k}',\omega)\rangle_{\mathbf{k}'} R(z,\omega) \tag{52}$$

with

$$R(z,\omega) = -2\pi i\left(b(\omega)+\frac{1}{2}\right) + \psi\left(\frac{1}{2}+i\,\frac{\omega - z}{2\pi T}\right) - \psi\left(\frac{1}{2}-i\,\frac{\omega+z}{2\pi T}\right), \tag{53}$$

$$\alpha^2 F(\mathbf{k},\mathbf{k}',\omega) = N(0)\sum_{\lambda} |g(\mathbf{k},\mathbf{k}-\mathbf{k}',\lambda)|^2 \times \delta(\omega - \omega(\mathbf{k}-\mathbf{k}',\lambda))\gamma^2(\mathbf{k},\mathbf{k}-\mathbf{k}'). \tag{54}$$

$b(\omega)$ denotes the Bose distribution and ψ the digamma function. $g(\mathbf{k},\mathbf{q},\lambda)$ is related to $g_i(\mathbf{q}\lambda)$ by a Fourier transform with respect to the site label i. $\langle\ \rangle_{\mathbf{k}}$ denotes a Fermi-surface average with respect to the momentum $\mathbf{k}$ and $N(0)$ is the density of renormalized particle states for one spin direction. In the one-particle approximation (i.e., if $U=0$) $\alpha^2 F$ is also given by Eq. (54) except for two important changes: $N(0)$ is replaced by the density of noninteracting particle states which is $N(0)$ multiplied by q_0. The second change concerns γ: in the free particle approximation $\gamma=1$ whereas in our case with $U=\infty$ γ is the momentum-dependent function Eq. (41).

Depending on the symmetry of the superconducting order parameter various averages of the above function $\alpha^2 F(\mathbf{k},\mathbf{k}',\omega)$ enter the Eliashberg equation. Assuming that the order parameter transforms according to the representation Γ_i of the point group C_{4v} of the square lattice the appropriate symmetry-projected function is

$$\alpha^2 F_i(\tilde{\mathbf{k}},\tilde{\mathbf{k}}',\omega) = N(0)\,\frac{1}{8}\sum_{\lambda,j} |g(\tilde{\mathbf{k}},\tilde{\mathbf{k}}-T_j\tilde{\mathbf{k}}',\lambda)|^2 \times \delta(\omega-\omega(\tilde{\mathbf{k}}-T_j\tilde{\mathbf{k}}',\lambda))\gamma^2(\tilde{\mathbf{k}},\tilde{\mathbf{k}}-T_j\tilde{\mathbf{k}}')D_i(j). \tag{55}$$

$\tilde{\mathbf{k}}$ and $\tilde{\mathbf{k}}'$ are momenta on the Fermi line in the irreducible Brillouin zone which is 1/8 of the total Brillouin zone. T_j, $j=1,..8$, denote the eight point-group transformations forming the symmetry group C_{4v} of a square lattice. This group has five irreducible representations which we distinguish by the label $i=1,2...5$. In the following the representations $i=1$ and $i=3$ will be of importance corresponding to s- and d-wave symmetry in the full rotation group. $D_i(j)$ is the representation matrix of the jth transformation for the representation i. Assuming that the order parameter does not vary much in the irreducible Brillouin zone one can average over $\tilde{\mathbf{k}}$ and $\tilde{\mathbf{k}}'$ in the irreducible Brillouin zone. For each symmetry one obtains in this way a function

$$\alpha^2 F_i(\omega) = \langle\langle \alpha^2 F_i(\tilde{\mathbf{k}},\tilde{\mathbf{k}}',\omega)\rangle_{\tilde{\mathbf{k}}}\rangle_{\tilde{\mathbf{k}}'} \tag{56}$$

which, in a first approximation, determines the transition temperature for an order parameter with symmetry Γ_i. Performing a similar calculation as above for the phonon-limited resistivity one finds that the resistivity is related to the function $\alpha^2_{\mathrm{tr}} F(\omega)$ as usual[30] and that $\alpha^2_{\mathrm{tr}} F(\omega)$ is given by

$$\alpha^2_{\mathrm{tr}} F(\omega) = \langle\langle \alpha^2 F(\mathbf{k},\mathbf{k}',\omega)[\mathbf{v}(\mathbf{k})-\mathbf{v}(\mathbf{k}')]^2\rangle_{\mathbf{k}}\rangle_{\mathbf{k}'} / (2\langle\langle \mathbf{v}^2(\mathbf{k})\rangle_{\mathbf{k}}\rangle_{\mathbf{k}'}). \tag{57}$$

The effect of correlations can be discussed in a simple way if one assumes that the bare coupling function $g(\mathbf{k},\mathbf{k}',\lambda)$ and the phonon frequencies $\omega(\mathbf{k},\lambda)$ are independent of momenta. Correlation effects in $\alpha^2 F_i$ at zero frequency are then described by the "enhancement" functions

$$\Lambda_i = \frac{1}{8}\sum_{j=1}^{8}\left\langle\left\langle \frac{|\gamma(\tilde{\mathbf{k}},\tilde{\mathbf{k}}-T_j\tilde{\mathbf{k}}')|^2}{q_0}\right\rangle_{\tilde{\mathbf{k}}}\right\rangle_{\tilde{\mathbf{k}}'} D_i(j). \tag{58}$$

Similarly, correlation effects in the resistivity ρ are described by $\delta\Lambda_{\mathrm{tr}}$ with

$$\Lambda_{\mathrm{tr}} = \left\langle\left\langle \frac{|\gamma(\mathbf{k},\mathbf{k}-\mathbf{k}')|^2}{q_0}[\mathbf{v}(\mathbf{k})-\mathbf{v}(\mathbf{k}')]^2\right\rangle_{\mathbf{k}}\right\rangle_{\mathbf{k}'} \Big/ (2\langle\langle \mathbf{v}^2(\mathbf{k})\rangle_{\mathbf{k}}\rangle_{\mathbf{k}'}). \tag{59}$$

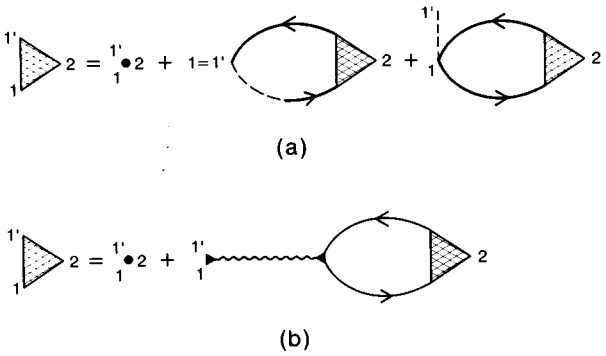

FIG. 1. Diagrammatic equation for the electron-phonon vertex (shaded triangle) using (a) Hubbard's X operators and (b) slave-boson theory. Fat solid, thin solid, and wavy lines denote electron, spinon, and boson propagators, the dashed line the hopping term, the small filled circles and triangles δ functions and the bare spinon-boson interaction, respectively.

The additional factor δ in ρ is due to the fact that ρ contains renormalized Fermi velocities (yielding a factor δ^2) as well as a density of state factor (yielding a factor $1/\delta$) so that altogether a factor δ appears in front of $\Lambda_{\rm tr}$. Absence of correlations implies that $\Lambda_1=\Lambda_{\rm tr}=1$, $\Lambda_i=0$ for $i>1$, and the absence of the factor δ in the relation between ρ and $\Lambda_{\rm tr}$.

V. COMPARISON WITH THE SLAVE-BOSON APPROACH

Comparison with Ref. 22 shows that our $O(1)$ result for $\Sigma^{(0)}$, Eq. (37), agrees exactly with the corresponding slave-boson result. Only the meaning of various quantities is different which is due to the fact that, for instance, there is no Bose condensate in our approach. In the following we will compare our expression for the vertex function γ, Eqs. (40)–(44), with that of slave-boson theory.

Figure 1(a) shows the vertex equation of the X-operator approach which has been used in Sec. IV. The corresponding vertex equation of the slave-boson approach is graphically shown in Fig. 1(b) and looks quite different from Fig. 1(a). The thin solid lines in Fig. 1(b) denote the spinon Green's function, the wavy line an effective potential due to fluctuations in the amplitude of the condensate and the variable conjugate to the constraint. The corresponding analytic expressions are[22,31]

$$\gamma(k,q)=1+\frac{1}{2}\sum_{k'} G(k')G(k'+q)v_{\rm eff}(k,k',q), \quad (60)$$

$$v_{\rm eff}(k,k',q)=\{-L_{rr}(q)+i[\epsilon(k')+\epsilon(k'+q)+\epsilon(k)+\epsilon(k+q)]L_{r\lambda}(q)+[\epsilon(k)+\epsilon(k+q)][\epsilon(k')+\epsilon(k'+q)]L_{\lambda\lambda}(q)\}/D(q), \quad (61)$$

$$D(q)=L_{rr}(q)L_{\lambda\lambda}(q)-L_{r\lambda}^2(q). \quad (62)$$

Comparing the expression for the L's in Ref. 22 with our expressions for a,b,c we find with $q=(\mathbf{q},i\nu_n)$

$$L_{\lambda\lambda}(q)=a(q)/2, \quad (63)$$

$$L_{r\lambda}(q)=-iq_0\{1+[b(q)+b(-q)]/2\}, \quad (64)$$

$$L_{rr}(q)=-2q_0^2c(q)+{\nu_n}^2a(q)/2. \quad (65)$$

Inserting Eqs. (61)–(65) into Eq. (60) we obtain

$$\gamma(k,q)=\frac{1+b(q)-a(q)[t(\mathbf{k})+t(\mathbf{k}+\mathbf{q})]/2}{[1+b(q)][1+b(-q)]-a(q)c(q)}. \quad (66)$$

The denominators in Eqs. (41) and (66) are the same which implies, for instance, that the collective excitations are the same in the two approaches. However, the numerator in Eq. (66) is somewhat different from that of Eq. (41): The slave-boson expression is symmetric in the initial and final momenta of electrons, $\mathbf{k}$ and $\mathbf{k}+\mathbf{q}$, respectively. In the expression of the X-operator approach only the initial momentum $\mathbf{k}$ appears. The origin and the relevance of this discrepancy between the two approaches are presently not well understood. Note, however, that this discrepancy vanishes in the limit $q\to 0$ and is also irrelevant in all cases where the electron momenta can be put right onto the Fermi surface. On the other hand, $\gamma(k,q)$ is the ratio of the renormalized and the bare electron-phonon coupling. Equivalent theories thus should give the same value for γ for arbitrary arguments k and q.

VI. RESULTS AND DISCUSSION

A. Limiting cases of the vertex function and the one-dimensional case

Keeping the frequency finite and taking the limit $\mathbf{q}\to 0$ Eqs. (42)–(44) yield $a=b=c\to 0$ and therefore $\gamma\to 1$. This limit is relevant for the renormalization of $\mathbf{q}=0$ phonons due to superconductivity. In these calculations the bare, unscreened vertex $\gamma=1$ should be used in agreement with Ref. 32.

A less trivial case is obtained if we first put the frequency to zero and then let $\mathbf{q}$ go to zero. From Eqs. (42)–(44) follows

$$a\to N(\mu), \quad (67)$$

$$b\to -\frac{\mu}{q_0}N(\mu), \quad (68)$$

$$c\to \frac{\mu^2}{q_0^2}N(\mu), \quad (69)$$

so that

$$\lim_{\mathbf{q}\to 0}\gamma(k_F,\mathbf{q},i\nu_n)=\frac{1}{1-2(\mu/q_0)N(\mu)}. \quad (70)$$

The denominator in Eq. (70) is related to the compressibility κ by

$$\kappa=\frac{N(\mu)}{1-2(\mu/q_0)N(\mu)}. \quad (71)$$

Near a boundary for phase separation κ diverges. According to Eq. (71) this may happen in two different ways: $N(\mu)$ diverges and, at the same time, $\mu\to 0$ which holds in the t model at half-filling; or, $N(\mu)$ remains finite but the denominator in Eq. (71) vanishes. This case occurs in the tt' model if $t/t'>0$. Real high-T_c oxides, however, always correspond to the case $t/t'<0$, so we will not consider the possibility $t/t'>0$ further.

In the following we assume that the adiabatic approximation holds so that the ω dependence of a, b, c, and γ can be neglected. The $\mathbf{k}$ integrals in a,b,c can be performed in general only numerically. However, in the special case of one dimension, these integrals can be carried out analytically. Putting $4t$ and a to one one obtains the following results:

$$a(q)=\frac{\sqrt{2}}{\pi\delta}\frac{1}{\sqrt{1-\cos(q)}}\ln\left|\frac{tg(|q|/4+k_F/2)}{tg(|q|/4-k_F/2)}\right|, \tag{72}$$

$$b(q)=\frac{1}{\pi\delta}\frac{\sin|q|}{1-\cos(q)}\ln\left|\frac{\sin(k_F+|q|/2)}{\sin(k_F-|q|/2)}\right|, \tag{73}$$

$$c(q)=\frac{2}{\pi\delta}[f(q)\cos(q)-g(q)\sin|q|], \tag{74}$$

with the two functions

$$f(q)=\sin(k_F)+\frac{1}{2}\,\mathrm{ctg}\left(\frac{|q|}{2}\right)\ln\left|\frac{\sin(k_F)+|\sin(q/2)|}{\sin(k_F)-|\sin(q/2)|}\right|, \tag{75}$$

$$g(q)=\mathrm{ctg}\left(\frac{|q|}{2}\right)\sin(k_F)-\frac{1}{4}\frac{\sin(q)}{|\sin(q/2)|}\ln\left|\frac{\sin(k_F)+|\sin(q/2)|}{\sin(k_F)-|\sin(q/2)|}\right|. \tag{76}$$

δ is the doping away from half-filling and related to k_F by $1-\delta=2k_F/\pi$. The renormalized energies are $\epsilon(k)=-q_0\cos(k)$ with $q_0=\delta/2$. Inserting Eqs. (72)–(75) into Eq. (41) yields an analytic expression for the vertex function γ. γ is an even function in q and periodic in q with period 2π so it is sufficient to vary q in the interval $[0,\pi]$. The $q\to 0$ limit of γ is

$$\lim_{q\to 0}\gamma(k_F,q)=\frac{1}{\{1+[4\cot(k_F)/(\pi-2k_F)]\}} \tag{77}$$

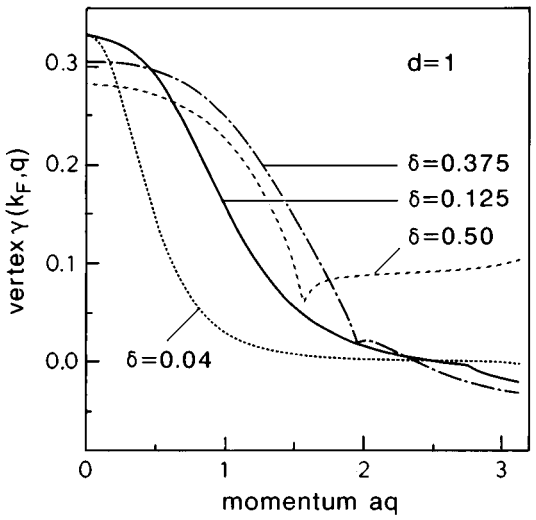

FIG. 2. Vertex function $\gamma(k_F,q)$ as a function of aq for four different dopings δ in the one-dimensional t model.

with approaches 1/3 for $\delta\to 0$ and ∞ for $\delta\to 1$. The compressibility κ, Eq. (71), becomes

$$\kappa=\frac{2}{\pi\delta\cos(\pi\delta/2)+2\sin(\pi\delta/2)} \tag{78}$$

and diverges for $\delta\to 0$. Since $\lim_{q\to 0}\gamma(k_F,q)$ and κ differ only by a density of states factor the divergence of κ is caused by the divergence of the density of states at half-filling.

Near $2k_F$ a,b,c, and γ behave as follows if $|k|<2k_F$:

$$a(2k_F-k)=\frac{1}{\pi\delta}\frac{1}{\sin(k_F)}\ln\left|\frac{1}{k}\right|, \tag{79}$$

$$b(2k_F-k)=\frac{1}{\pi\delta}\cot(k_F)\ln\left|\frac{1}{k}\right|, \tag{80}$$

$$c(2k_F-k)=\frac{1}{\pi\delta}[\cot(k_F)\cos(2k_F)+\cos(k_F)\sin(2k_F)]\ln\left|\frac{1}{k}\right|, \tag{81}$$

$$\gamma(2k_F-k)=\frac{\pi\delta\tan(k_F)}{\ln|1/k|}\frac{1+2\cos(k_F)}{1-2\cos^2(k_F)}. \tag{82}$$

Each of the three susceptibilities a,b,c diverges at $2k_F$ and is symmetric with respect to $2k_F$. The vertex function, on the other hand, approaches zero at $2k_F$ in a logarithmically way from above for $\cos(k_F)<1/\sqrt{2}$ and from below for $\cos(k_F)>1/\sqrt{2}$. This implies that for $\cos(k_F)>1/\sqrt{2}$, γ changes from positive values at small momenta to negative values at large momenta at a momentum which is somewhat smaller than $2k_F$.

Figure 2 shows plots for γ as a function of q for four different values of the doping. Expanding Eqs. (72)–(74) for small δ's and q's yields the approximate expression

$$\gamma\sim\frac{1}{3+q^2/(6\pi^2\delta^2)}. \tag{83}$$

γ thus approaches for small δ's a Lorentzian with height 1/3 and width $3\pi\delta\sqrt{2}$, in agreement with Fig. 2. For $\delta=0.125$ the logarithmic singularity at $2k_F$ becomes visible in the plot at $aq\sim 2.7$ in the form of a small change in the slope. Increasing the doping the $2k_F$ singularity moves to smaller momenta, becomes more pronounced, and changes its sign in agreement with Eq. (82). γ is always a strongly decreasing function for $q<2k_F$ but beyond $2k_F$ it starts to increase with increasing momentum if $\delta>0.5$. In the next section we will find that some of these features are also typical for the two-dimensional case.

B. Results for the t and tt' models on a square lattice

As discussed in Sec. IV the renormalized band for electrons in $O(1)$ is given by

$$\epsilon(\mathbf{k})=-q_0[\cos(k_x a)+\cos(k_y a)+8t'\cos(k_x a)\cos(k_y a)] \tag{84}$$

with $q_0=\delta/2$ and measuring all energies in units of $4t$. There is in addition a constant, doping-dependent term on the right-hand side of Eq. (84) due to the first term in Eq. (37). It will play no role in the following so we will drop it for simplicity.

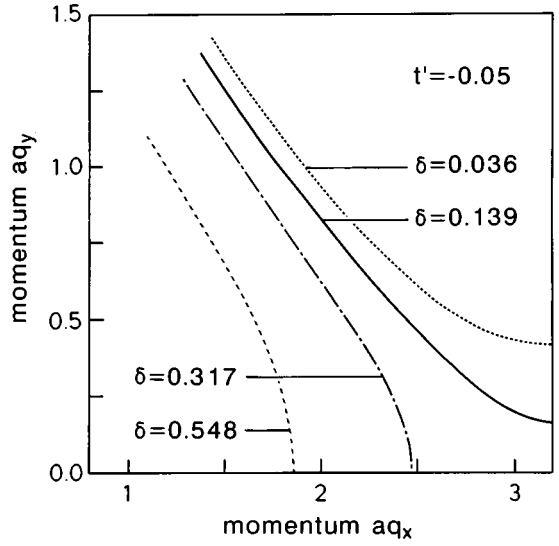

FIG. 3. Fermi lines in the irreducible Brillouin zone for four different dopings δ and $t'=-0.05$ in units of $4t$.

Typical values for t' are $t'\sim-0.125$ for $YBa_2Cu_3O_7$ and ~-0.05 for maximal doped La_2CuO_4. Figure 3 shows Fermi lines in the irreducible part of the Brillouin zone for $t'=-0.05$ for different values of the chemical potential: For $\mu>4q_0t'$ the Fermi lines are centered around the M point; at $\mu=4q_0t'$ there is a van Hove singularity, and for $\mu<4q_0t'$ the lines are centered around the Γ point. The density of states can be obtained analytically after a lengthy but elementary calculation:

$$N(\mu)=\frac{1}{\pi^2 q_0\sqrt{1-8\tilde{\mu}t'}}\,K\left(\frac{4-(\tilde{\mu}+8t')^2}{4(1-8\tilde{\mu}t')}\right) \qquad (85)$$

with $\tilde{\mu}=\mu/q_0$. K is the elliptic function of the first kind. For $\tilde{\mu}<-2-4t'$ the band is empty and the maximum occupation is reached already at negative values for $\tilde{\mu}$ if t' is negative. All subsequent calculations for the tt' model are carried

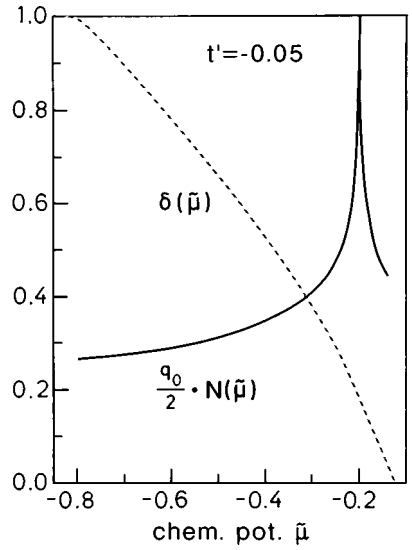

FIG. 4. Density of states $(q_0/2)\cdot N(\tilde{\mu})$ and the mean site occupation $\delta(\tilde{\mu})$ as a function of the renormalized chemical potential $\tilde{\mu}$ for $t'=-0.05$.

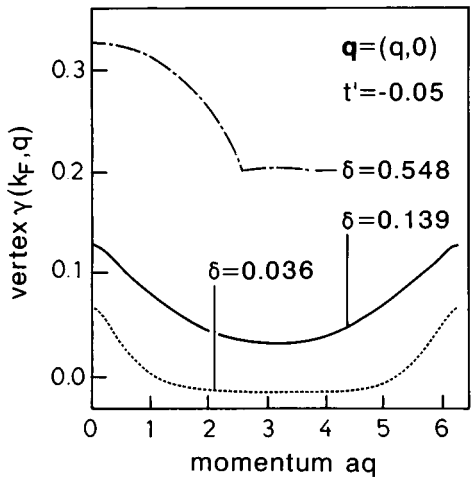

FIG. 5. Vertex $\gamma(k_F,q)$ as a function of the momentum aq with $\mathbf{q}=(q,0)$ for $t'=-0.05$.

out for $t'=-0.05$ where the maximal occupation, i.e., $\delta=0$, is reached at $\tilde{\mu}=-0.12$. The density $(q_0/2)N(\tilde{\mu})$ as well as the average occupation per site, $\delta(\tilde{\mu})$, are shown in Fig. 4 as solid and broken lines, respectively. The peak in $N(\tilde{\mu})$ at $\tilde{\mu}=-0.2$ is caused by the van Hove singularity.

The vertex function $\gamma(\mathbf{k},\mathbf{q})$ depends on $\mathbf{k}$ only via $t(\mathbf{k})$, i.e., only via the Fermi energy. The first argument is therefore constant for a given doping, denoted symbolically by k_F in the following. γ as a function of $\mathbf{q}$ is only restricted by the point group of the square lattice, i.e., it still depends in general on the direction of $\mathbf{q}$. Plots of γ as a function of momentum along the [10] and the [11] directions have been presented in Refs. 18, 26, and 27 for the t model. These results also agree with the slave-boson method I of Ref. 33. The second slave-boson method II in that reference which is not based on a $1/N$ expansion gives comparable results for large momentum but much smaller values for small momentum transfers. Figures 5 and 6 show similar plots for γ for the tt' model. For each doping δ the momentum q varies between 0 and the largest possible momentum transfer on the Fermi surface. At large δ's γ is rather unaffected by t'. For smaller dopings the tt' model shows two new features compared to

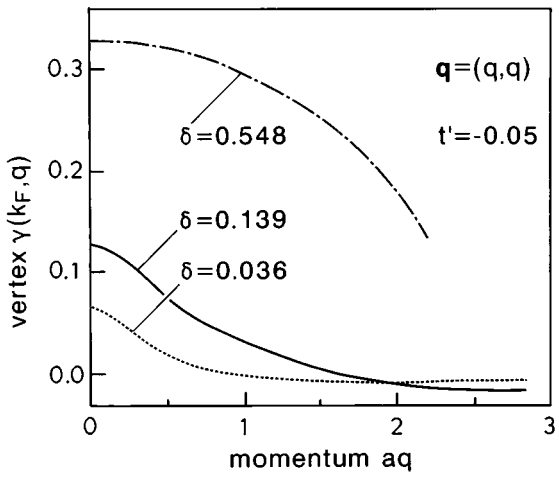

FIG. 6. Vertex $\gamma(k_F,q)$ as a function of the momentum aq with $\mathbf{q}=(q,q)$ for $t'=-0.05$.

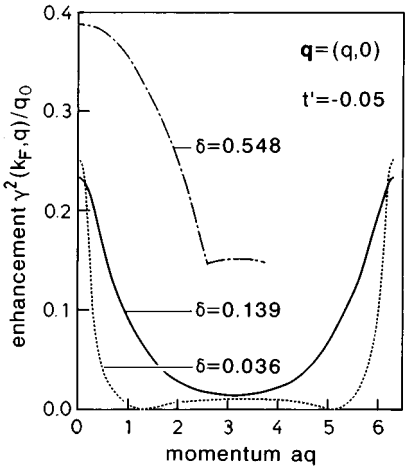

FIG. 7. Enhancement function $\gamma^2(k_F,q)/q_0$ as a function of the momentum aq with $\mathbf{q}=(q,0)$ for $t'=-0.05$.

the t model: The absolute values for γ are substantially reduced which can be verified analytically in the limit $\mathbf{q}\to 0$ using Eq. (85); γ may become slightly negative at larger momenta similar as in the one-dimensional case. The most important features of γ in the t model do, however, not change in the tt' model: γ depends for not too large dopings strongly on the momentum and decreases monotonically with increasing momentum. At larger momenta and small dopings γ becomes very small which implies that also the effective electron-phonon coupling becomes very small in this region even if the bare coupling was large.

Figures 7 and 8 show the enhancement function $\gamma^2(k_F,\mathbf{q})/q_0$ for the tt' model as a function of $\mathbf{q}$ between 0 and $2k_F$ along the [10] and [11] directions, respectively. Similarly to the t model this function is strongly $\mathbf{q}$ dependent for not too large dopings, decreases monotonically with q, and assumes in general very small values at large momenta and small dopings. For the special case of the [10] direction the enhancement function increases again at large momenta and small dopings due to the symmetry requirement that it has to be symmetric with respect to π. Compared to the t

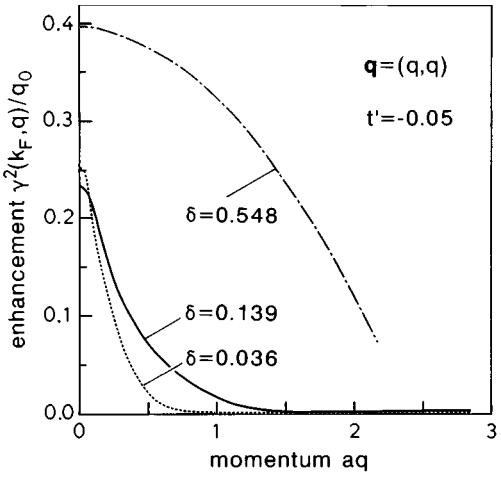

FIG. 8. Enhancement function $\gamma^2(k_F,q)/q_0$ as a function of the momentum aq with $\mathbf{q}=(q,q)$ for $t'=-0.05$.

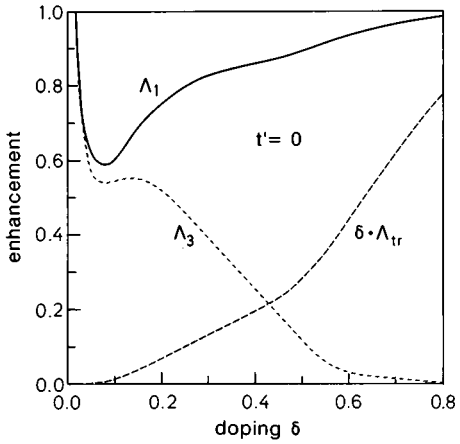

FIG. 9. Enhancements Λ_1, Λ_3, and $\delta\Lambda_{\rm tr}$ as a function of doping δ for the t model.

model the enhancement function of the tt' model shows smaller absolute values and the increase towards $q=0$ is less dramatic.

As discussed at the end of Sec. IV the enhancement functions Λ_1 and $\Lambda_{\rm tr}$ describe the change in α^2F_i and $\alpha^2_{\rm tr}F$, respectively, due to correlations if the $\mathbf{q}$ dependence of the bare electron-phonon interaction and the phonon branches can be neglected. Approximating the Fermi surface by a cylinder Λ_1 becomes

$$\Lambda_1=\int d^2q\langle\langle\delta(\mathbf{q}-\mathbf{p}+\mathbf{p}')\rangle_{\mathbf{p}}\rangle_{\mathbf{p}'}\gamma^2(k_F,\mathbf{q})/q_0. \quad (86)$$

A straightforward calculation gives in two dimensions

$$\langle\langle\delta(\mathbf{q}-\mathbf{p}+\mathbf{p}')\rangle_{\mathbf{p}}\rangle_{\mathbf{p}'}=\frac{1}{\pi^2 q}\frac{\Theta(2k_F-q)\Theta(q)}{\sqrt{4k_F^2-q^2}}, \quad (87)$$

so that

$$\Lambda_1=\frac{2}{\pi}\int_0^{2k_F}dq\,\frac{1}{\sqrt{4k_F^2-q^2}}\frac{\gamma^2(k_F,q)}{q_0}, \quad (88)$$

assuming also that γ depends only on $|\mathbf{q}|$. Λ_1 is thus given by a slightly distorted average of $\gamma^2(k_F,q)/q_0$ between 0 and $2k_F$. Similarly, $\Lambda_{\rm tr}$ is given by Eq. (88) if the additional factor $q^2/(2k_F^2)$ is inserted in the integrand. The effect of the strong $\mathbf{q}$ dependence of γ^2/q_0 is now evident from Figs. 7 and 8: In Λ_1 both small and large momentum transfers are important whereas only large momenta contribute to $\Lambda_{\rm tr}$. As a result $\Lambda_{\rm tr}$ will decrease much stronger than Λ_1 with decreasing δ. One expects therefore a substantial difference between Λ_1 and $\Lambda_{\rm tr}$ at small dopings caused by the strong momentum dependence of the vertex function and thus by correlations.

We have performed the averages in Λ_1, Λ_3, and $\Lambda_{\rm tr}$ numerically using the true anisotropic band dispersion and vertex. Figures 9 and 10 show the results for the t and the tt' models, respectively. We have multiplied the three curves with a common factor so that Λ_1 approaches 1 in the empty-band limit $\delta\to 1$. We also have plotted $\delta\Lambda_{\rm tr}$ instead of $\Lambda_{\rm tr}$ because the doping dependence of the resistivity is given by $\delta\Lambda_{\rm tr}$ as discussed at the end of Sec. IV. In the t model Λ_1

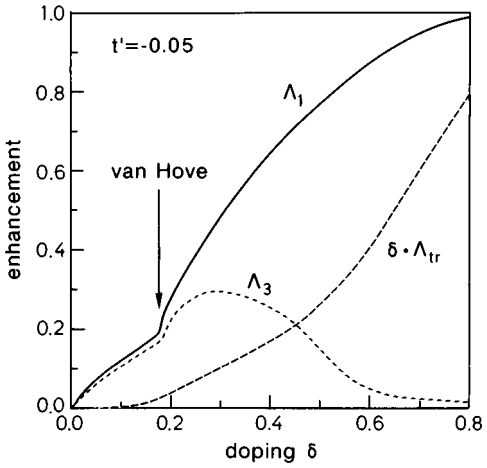

FIG. 10. Enhancements Λ_1, Λ_3, and $\delta\Lambda_{\rm tr}$ as a function of doping δ for $t'=-0.05$.

decreases first rather slowly with decreasing doping, passes through a minimum at $\delta\sim 0.1$ and then increases strongly at very small dopings. The asymptotic behavior of Λ_1 at small δ can be obtained analytically from Eq. (58): For a small δ $\gamma^2(k_F,q)/q_0$ has a width $\sim\delta$ and a height $\sim 1/\delta$. Performing the averages in Eq. (58) one finds $\Lambda_1\sim 1/\delta$ in agreement with the numerical result. The decrease of Λ_1 with decreasing δ is much stronger in the case of the tt' model: Between $\delta=1$ and $\delta=0.2$ Λ_1 decreases roughly by a factor 5. The van Hove singularity at $\delta\sim 0.17$ is clearly visible in Λ_1 producing a change in the slope at the singularity. For $\delta\rightarrow 0$ Λ_1 approaches 0 in the tt' model because γ approaches 0 in this limit. The different limits of the t and the tt' models for $\delta\rightarrow 0$ are due to the fact that the density of states diverges in the t, but not in the tt' model in this limit. Since Λ_1 is the effective coupling constant for s-wave pairing one concludes that correlation effects suppress T_c in a monotonous way as function of doping and that this suppression is rather small in the case of the t, but substantial for the tt' model. The authors of Ref. 31 argued for a rather different behavior: T_c should show a maximum at small dopings and not be much suppressed by correlations. It is presently unclear whether the different behaviors of T_c can be attributed solely to the different electron-phonon coupling (modulation of the hopping matrix elements by core displacements) used in Ref. 31.

The short-dashed lines in Figs. 9 and 10 show the doping dependence of Λ_3 which is responsible for d-wave superconductivity. Λ_3 must vanish for $\delta\rightarrow 1$ because we assumed a **q**-independent bare electron-phonon coupling and dispersionless phonon branches. With decreasing δ the function $\gamma^2(k_F,q)/q_0$ becomes more and more **q** dependent leading to a finite Λ_3. The unaveraged effective interaction has always the same sign in **q** space which implies $\Lambda_1>\Lambda_3$. The equality sign occurs exactly then if the effective interaction is diagonal in **q** space so that it no longer scatters electrons between different momentum states on the Fermi surface. This situation occurs approximately at small dopings where the function $\gamma^2(k_F,q)/q_0$ develops a very narrow forward scattering peak. As a result Λ_3 is nearly coincident with Λ_1 at small dopings. In the t model Λ_3 diverges similar to Λ_1 at small dopings. In the tt' model, on the other hand, Λ_3 always has a maximum in the region of small or intermediate dopings. Taking also Coulomb repulsion into account Λ_1, but not Λ_3, will be suppressed within the usual approximation. Thus d-wave superconductivity necessarily becomes more stable than s-wave superconductivity at sufficiently small dopings in both models. This transition from s- to d-wave superconductivity is caused entirely by electronic correlations because our bare electron-phonon coupling is assumed to have only s-wave symmetry.

The long-dashed lines in Figs. 9 and 10 describe $\delta\Lambda_{\rm tr}$. Both in the t and the tt' models $\delta\Lambda_{\rm tr}$ decreases very fast with decreasing δ and is very small for $\delta<0.4$. The quenching of $\delta\Lambda_{\rm tr}$ is caused by two effects: First, $\gamma^2(k_F,q)/q_0$ becomes with decreasing δ very small for large momenta and large for small momenta. Due to the factor $[\mathbf{v}(\mathbf{k})-\mathbf{v}(\mathbf{k}')]^2$ in $\Lambda_{\rm tr}$ only large momentum transfers contribute to $\Lambda_{\rm tr}$ which decrease $\Lambda_{\rm tr}$. Second, the Fermi velocities entering $\Lambda_{\rm tr}$ are renormalized ones leading, together with a density of states factor to a factor δ in the resistivity ρ which suppresses ρ at small dopings. As a net result correlation effects quench $\Lambda_{\rm tr}$ by about one order of magnitude in the small or intermediate doping regime. The electrons are then only weakly scattered by phonons or, using similar arguments, by impurities and the electron-phonon interaction becomes rather ineffective due to correlation effects.

VII. CONCLUSIONS

In the preceding sections we have calculated the renormalization of the electron-phonon interaction by strong electronic correlations. For this we used an infinite-U Hubbard model with nearest- and second-nearest-neighbor hopping terms on a square lattice and an electron-phonon coupling where the phonons couple to density fluctuations on the atoms. Our results for the various symmetry components of the Eliashberg function α^2F and the corresponding transport function $\alpha^2_{\rm tr}F$ are asymptotically exact at large N and for a small electron-phonon coupling constant. Useful quantities characterizing the correlation effects are the enhancement functions Λ_i. They are defined as the ratio of α^2F_i at doping δ and at $\delta=1$ taken at zero frequency and for the symmetry component i. If the momentum dependence of the bare electron-phonon coupling and of the phonon branches can be neglected Λ_i renormalizes the α^2F_i or λ_i of the uncorrelated case in a multiplicative way.

We find that electronic correlations affect different symmetry components of α^2F in a different way: The totally symmetric function Λ_1 in general decreases with decreasing doping with the biggest effects occurring at small dopings. In the t model the reduction is rather moderate except at very small dopings where Λ_1 even increases and diverges due to the coincidence of the van Hove singularity and the metal-insulator transition at half-filling. For the more realistic tt' model the correlation-induced reduction of Λ_1 is monotonous as function of δ and quite large for small dopings. Our numerical results suggest that electronic correlations suppress in general phonon pairing, especially in the tt' model, at least in the adiabatic approximation, i.e., for $\omega<\mathbf{k}\cdot\mathbf{v_F}(\mathbf{k})$. In the nonadiabatic regime $\omega>\mathbf{k}\cdot\mathbf{v_F}(\mathbf{k})$ the enhancement function $\gamma^2(k_F,q)/q_0$ may be substantially larger compared to the adiabatic case because γ tends to the bare value 1. A proper inclusion of these effects in a T_c calculation would

need a solution of Eliashberg equations taking into account the energy dependence of the vertex at small dopings and of the density of states near the van Hove singularity.

Another correlation effect is that the nontrivial symmetries Λ_i with $i>1$ can no longer be disregarded. In our calculations we assumed that the bare electron-phonon coupling has only a s-wave component $i=1$. Therefore all functions Λ_i with $i>1$ have to vanish in the empty band case $\delta\rightarrow 1$. With decreasing doping the vertex becomes momentum dependent and develops a forward scattering peak at small dopings. As a result functions Λ_i are nonzero and of similar magnitude and approach the same value in the limit of vanishing doping. We have verified this for the d-wave-like component Λ_3 by numerical calculations. In both models Λ_3 indeed approaches Λ_1 from below at small dopings; in the tt' model Λ_3 vanishes for $\delta\rightarrow 0$ and $\delta\rightarrow 1$ and shows a maximum near the van Hove singularity. Taking also the direct Coulomb repulsion into account it was argued that for our models a s-wave order parameter can never be the stable order parameter below a certain critical value for the doping. This result is remarkable because it holds for phonon-mediated superconductivity and it is asymptotically exact at large N and for a small electron-phonon coupling.

Finally we find that the doping-dependent part of the resistivity, $\delta\Lambda_{\mathrm{tr}}$, is heavily suppressed by correlations, both in the t and the tt' models at low and intermediate dopings. This is a consequence of the appearance of a forward scattering peak in the vertex function in this regime. Our results suggest that this feature is a generic one for strongly correlated systems. Moreover, they are consistent with the experimental observation that the transport coefficients in high-T_c oxides do not exhibit features which are characteristic for the electron-phonon scattering.

ACKNOWLEDGMENTS

It is a pleasure for the authors to thank L. Gehlhoff and A. Greco for many discussions. Helpful remarks of I. Mazin concerning vertex corrections are also acknowledged. One of us (M.L.K.) would like to thank Professor M. Mehring for support. He also acknowledges the hospitality of the University of Stuttgart and the Max-Planck-Institut für Festkörperforschung.

[1] M. Schlüter and M. S. Hybertsen, Physica C **162-164**, 583 (1989).
[2] H. Eskes, G. A. Sawatzki, and L. F. Feiner, Physica C **160**, 424 (1989).
[3] G. Mante, R. Claessen, A. Huss, R. Manzke, M. Skibowski, Th. Wolf, M. Knupfer, and J. Fink, Phys. Rev. B **44**, 9500 (1991).
[4] D. B. Tanner and T. Timusk, in *Physical Properties of High Temperature Superconductors III*, edited by D. M. Ginsberg (World Scientific, Singapore, 1992), p. 363.
[5] S. Uchida, T. Ido, H. Takagi, T. Arima, and Y. Tokura, Phys. Rev. B **43**, 7942 (1991).
[6] O. K. Andersen, A. I. Liechtenstein, O. Rodriguez, I. I. Mazin, O. Jepsen, V. P. Antropov, O. Gunnarsson, and S. Golopan, Physica C **185-189**, 147 (1991).
[7] H. Krakauer, W. E. Pickett, and R. E. Cohen, Phys. Rev. B **47**, 1002 (1993).
[8] C. Thomsen and M. Cardona, in *Physical Properties of High Temperature Superconductors I*, edited by D. M. Ginsberg (World Scientific, Singapore, 1989), p. 409.
[9] C. Frank, in *Physical Properties of High Temperature Superconductors IV*, edited by D. M. Ginsberg (World Scientific, Singapore, 1993), p. 189.
[10] S. I. Vedeneev, P. Samuely, S. V. Meshkov, G. M. Eliashberg, A. G. M. Jansen, and P. Wyder, Physica C **198**, 47 (1992).
[11] N. Miyakawa, Y. Shiina, T. Kaneko, and N. Tsuda, J. Phys. Soc. Jpn. **62**, 2445 (1993).
[12] R. Zeyher, Phys. Rev. B **44**, 10 404 (1991).
[13] S. Martin, A. T. Fiory, R. M. Fleming, L. F. Schneemeyer, and J. V. Waszczak, Phys. Rev. B **41**, 846 (1990).
[14] H. Takagi, B. Batlogg, H. L. Kao, J. Kwo, R. J. Cava, J. J. Krajewski, and W. F. Peck, Jr., Phys. Rev. Lett. **69**, 2975 (1992).
[15] R. Zeyher, J. Supercond. **7**, 537 (1994).
[16] Ju H. Kim, K. Levin, R. Wentzcovitsch, and A. Auerbach, Phys. Rev. B **44**, 5148 (1991).
[17] Ju H. Kim, K. Levin, R. Wentzcovitsch, and A. Auerbach, Phys. Rev. B **40**, 11 378 (1989).
[18] M. L. Kulić and R. Zeyher, Phys. Rev. B **49**, 4395 (1994).
[19] M. Grilli and C. Castellani, Phys. Rev. B **50**, 16 880 (1994).
[20] T. Tohyama, P. Horsch, and S. Maekawa, Phys. Rev. Lett. **74**, 980 (1995).
[21] R. Zeyher, Z. Phys. B **80**, 187 (1990).
[22] G. Kotliar and J. Liu, Phys. Rev. Lett. **61**, 1784 (1988).
[23] A. Houghton and A. Sudbo, Phys. Rev. B **38**, 7037 (1988).
[24] M. Grilli, C. Castellani, and C. Di Castro, Phys. Rev. B **42**, 6233 (1990).
[25] A. E. Ruckenstein and S. Schmitt-Rink, Phys. Rev. B **38**, 7188 (1988).
[26] R. Zeyher and M. L. Kulić, Physica B **199-200**, 358 (1994).
[27] R. Zeyher and M. L. Kulić, Physica C **235-240**, 2151 (1994).
[28] G. Baym and L. Kadanoff̂, Phys. Rev. B **124**, 287 (1961).
[29] P. B. Allen and B. Mitrović, *Solid State Physics: Advances in Research and Applications*, edited by H. Ehrenreich, F. Seitz, and D. Turnbull (Academic, New York, 1982), Vol. 37, p. 1.
[30] G. D. Mahan, *Many-Particle Physics* (Plenum, New York, 1981).
[31] J. H. Kim and Z. Tesanovic, Phys. Rev. Lett. **71**, 4218 (1993).
[32] R. Zeyher and G. Zwicknagl, Z. Phys. B **78**, 175 (1990).
[33] J. Keller, C. E. Leal, and F. Forsthofer, Physica B **206-207**, 739 (1995).
[34] L. Gehlhoff, Ph. D. thesis, University of Stuttgart, 1995.